

A numerical study on optimal FTMD parameters considering soil-structure interaction effects

Sadegh Etedali*¹, Mohammad Seifi^a and Morteza Akbari^b

¹Department of Civil Engineering, Birjand University of Technology, P.O. Box 97175-569, Birjand, Iran

(Received December 29, 2017, Revised September 5, 2018, Accepted September 28, 2018)

Abstract. The study on the performance of the nonlinear friction tuned mass dampers (FTMD) for the mitigation of the seismic responses of the structures is a topic that still inspires the efforts of researchers. The present paper aims to carry out a numerical study on the optimum tuning of TMD and FTMD parameters using a multi-objective particle swarm optimization (MOPSO) algorithm including soil-structure interaction (SSI) effects for seismic applications. Considering a 3-story structure, the performances of the optimized TMD and FTMD are compared with the uncontrolled structure for three types of soils and the fixed base state. The simulation results indicate that, unlike TMDs, optimum tuning of FTMD parameters for a large preselected mass ratio may not provide a best and optimum design. For low mass ratios, optimal selection of friction coefficient has an important key to enhance the performance of FTMDs. Consequently, a free parameter search of all FTMD parameters provides a better performance in comparison with considering a preselected mass ratio for FTMD in the optimum design stage of the FTMD. Furthermore, the SSI significant effects on the optimum design of the TMD and FTMD. The simulation results also show that the FTMD provides a better performance in reducing the maximum top floor displacement and acceleration of the building in different soil types. Moreover, the performance of the TMD and FTMD decrease with increasing soil softness, so that ignoring the SSI effects in the design process may give an incorrect and unrealistic estimation of their performance.

Keywords: seismic-excited structures; tuned mass damper; friction tuned mass damper; multi-objective particle swarm optimization; soil-structure interaction

1. Introduction

In recent years, structural control systems have been successfully developed for vibration mitigation of structures against dynamic loads such as strong wind and earthquake excitations. The traditional linear tuned mass damper (TMD) system is one of the common passive control systems to control vibration in the mechanical and structural application. The TMD system consists of a mass, a linear spring, and a viscous dashpot. Optimum tuning of these parameters has a direct effect on the responses of the main system (Warburton 1982). Therefore, some researchers applied the numerical methods (Tsai and Lin 1993, Sadek *et al.* 1997, Chang 1999, Bakre and Jangid 2007, Salvi and Rizzi 2012, Brzeski *et al.* 2016, Keshtegar and Etedali 2017) and metaheuristic optimization algorithms (Hadi and Arfiadi 1998, Lee *et al.* 2006, Leung and Zhang 2009, Kaveh *et al.* 2015, Etedali and Mollayi 2017) to perform parametric studies and optimum tuning of the TMD parameters. In the presence of uncertainties of the model, the optimum design of TMD parameters is addressed in

(Gholizad and Ojaghzadeh Mohammadi 2017, Lin *et al.* 2017). The TMD frequency is often tuned with a vibration frequency close to the first natural frequency of the main structure (Etedali and Tavakoli 2017), whereas SSI effects modify the characteristics of the main structure such as natural frequencies, damping ratios, and shape modes (Shourestani *et al.* 2018). Since the performance of the structures equipped with TMD is often studied based on the rigid base assumption without considering SSI effects, some studies recently are focused on the SSI effects on the performance and time responses of the structures equipped with TMD (Farshidianfar and Soheili 2013, Bekdas and Nighdeli 2107, Khatibinia *et al.* 2016).

In order to enhance the performance of TMD in the seismic application, active and semi-active TMD have also been considered in some studies (Heidari *et al.* 2016, Etedali *et al.* 2013, Etedali *et al.* 2018), nevertheless, complexity and the high cost of the devices, researchers have led to improving the efficiency of existing passive TMD systems. Energy dissipation using friction dampers is an effective strategy for mitigation of seismic vibrations of the structures. In order to enhance the performance of TMDs, a combined system of the traditional linear TMD with the idea of friction damper, namely FTMD, is proposed that in fact, it represents a nonlinear TMD system. Although many attempts have been made to investigate the design and application of traditional linear TMDs, the study on the nonlinear TMDs is still in the developmental stage. Ricciardelli and Vickery (1999) investigated the harmonic

*Corresponding author, Associate Professor
E-mail: etedali@birjandut.ac.ir

^aM.Sc., Independent Researcher
E-mail: mohammad_seifi71@yahoo.com

^bM.Sc., Independent Researcher
E-mail: akbari69.project@gmail.com

response of a single-degree-of-freedom (SDOF) system equipped with a TMD with linear stiffness and dry friction damping. Gewei and Basu (2011) used a statistical linearization method to replace the nonlinear friction of an FTMD by an equivalent viscous damping. They applied the statistical linearized solution to analyze dynamic characteristics of a structure-FTMD system. Pisal and Jangid (2014) investigated the performance of multiple friction tuned mass dampers in comparison with a single FTMD.

The slip force of the FTMD as a passive device is typically a constant value. If the slip force is tuned too large, the FTMD will not be able to slide and waste the energy for weak or moderate earthquakes. One way to overcome this disadvantage is to lower the slip force level of the FTMD. In this case, due to a small sliding force, the dampers will not be able to waste enough energy for strong earthquakes. Hence, design the slip force level of the FTMDs is a crucial and difficult issue for the designer. On the other hand, passive friction devices usually reduce the displacement of floors at the cost of an increase in the acceleration of floors. A good trade-off between the conflicted structural responses can be created using a meta-heuristic multi-objective optimization algorithm. Moreover, the previous studies indicate the seismic behavior of structures is significantly affected by the soil-structure interaction. The SSI effects significantly modify the dynamic characteristics of the structures, while considering the rigid base assumption for the structures; these changes have been ignored in the design process of the FTMDs. Nevertheless, there is no comprehensive parametric study on the optimum FTMD parameters including soil-structure interaction effects. The present paper aims to investigate the SSI effects on seismic performance of the structures equipped with FTMD. For this purpose, the seismic performance of a three-story structure in three cases of the uncontrolled structure, the structure equipped with TMD, and the structure equipped with FTMD are considered. The governing differential equations of motion of the structures including SSI effects are formulated for time history analyses of the structure subjected to earthquake excitations. In addition to the fixed base case, three types of soils include of soft, medium and dense soils are considered for investigation the SSI effects on performances TMD and FTMD. A parametric study is conducted on optimum TMD/FTMD parameters include of frequency ratio, damping ratio and friction coefficient for a vast and practical range of the TMD/FTMD mass ratio. A MOPSO algorithm as a powerful tool is employed for optimum tuning of the FTMD parameters and the influences of the optimum parameters of TMD and FTMD on seismic performance of the structure are studied for different conditions of ground state. At the end, the performances of TMD and FTMD are compared for the structure subjected to four well-known earthquake excitations.

The remainder of the paper is organized as follows. Section 2 developed the mathematical model of a structure equipped with an FTMD including SSI effects. An overview of MOPSO algorithm is introduced in Sections 3. The parametric and numerical studies are carried out on a three-story building equipped with an FTMD in section 4.

The simulation results are discussed in Section 5. The concluding remarks are summarized in Section 6.

2. Mathematical models

A linear three-story structure subjected to ground acceleration, $\ddot{u}_g(t)$, is assumed. Considering an FTMD situated on the top floor of the structure, only the degree-of-freedom of the main structure is added by one. Fig. 1 shows the ideal mathematical models of the structure equipped with a FTMD for two cases: a) without SSI effects and b) including SSI effects, which is considered for numerical studies. The governing dynamic equations of the seismic-excited structure equipped with FTMD in two cases are developed for the both without and with SSI effects in this Section.

2.1 Dynamic equations of motion for a seismic-excited structure equipped with an FTMD

The equation on motion of the structure for the case of without SSI effects can be written as

$$m\ddot{\mathbf{x}}(t) + c\dot{\mathbf{x}}(t) + k\mathbf{x}(t) = -m\mathbf{r}\ddot{u}_g(t) + bF_s \quad (1)$$

where m , c , and k represent the mass, damping, and stiffness matrices of the structural system, respectively. Also, r and b are the location vectors for the seismic excitation and friction force, respectively. $\mathbf{x}(t)$, $\dot{\mathbf{x}}(t)$ and $\ddot{\mathbf{x}}(t)$ are the relative displacement, velocity and acceleration vectors, respectively. Considering the studied structure, they are defined as follows

$$m = \begin{bmatrix} M_1 & 0 & 0 & 0 \\ 0 & M_2 & 0 & 0 \\ 0 & 0 & M_3 & 0 \\ 0 & 0 & 0 & M_{FTMD} \end{bmatrix} \quad (2)$$

$$c = \begin{bmatrix} C_1 + C_2 & -C_2 & 0 & 0 \\ -C_2 & C_2 + C_3 & -C_3 & 0 \\ 0 & -C_3 & C_3 + C_{FTMD} & -C_{FTMD} \\ 0 & 0 & -C_{FTMD} & C_{FTMD} \end{bmatrix} \quad (3)$$

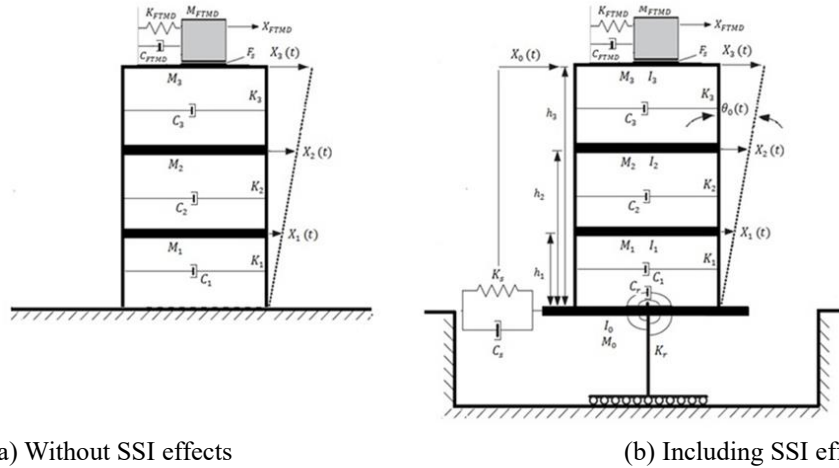
$$k = \begin{bmatrix} K_1 + K_2 & -K_2 & 0 & 0 \\ -K_2 & K_2 + K_3 & -K_3 & 0 \\ 0 & -K_3 & K_3 + K_{FTMD} & -K_{FTMD} \\ 0 & 0 & -K_{FTMD} & K_{FTMD} \end{bmatrix} \quad (4)$$

$$r = [1, 1, 1, 1]^T \quad (5)$$

$$b = [0, 0, -1, 1]^T \quad (6)$$

$$\mathbf{x}(t) = [X_1(t), X_2(t), X_3(t), X_{FTMD}(t)]^T \quad (7)$$

where M_i , C_i and K_i ($i=1,2,3$) represent respectively the mass, damping and stiffness of the i^{th} floor. Also, the FTMD parameters include of M_{FTMD} , C_{FTMD} and K_{FTMD} , represent the mass, damping and stiffness of the FTMD system. Furthermore, $X_i(t)$ is the relative displacement of the i^{th} floor and $X_{FTMD}(t)$ is the relative displacement of the FTMD system. In Eq. (1), the friction force of the



(a) Without SSI effects (b) Including SSI effects
Fig. 1 The mathematical models of the seismic-excited structure equipped with FTMD

FTMD, F_s , is given by the following equation

$$F_s = f_s \text{sgn}(\dot{X}_{FTMD} - \dot{X}_3) \quad (8)$$

where \dot{X}_{FTMD} is the velocity of the FTMD and \dot{X}_3 denotes the velocity of the top story. Using the hysteretic model proposed by Constantinou *et al.* (1990) and Wen's equation (1976), the damper force is given by the following equation

$$F_s = f_s Z \quad (9)$$

where f_s represents the limiting friction force or slip force of the damper and Z is the non-dimensional hysteretic component, which satisfies the following first-order non-linear differential equation.

$$q \frac{dz}{dt} = A(\dot{X}_{FTMD} - \dot{X}_3) - \beta |\dot{X}_{FTMD} - \dot{X}_3| Z |Z|^{n-1} - \tau (\dot{X}_{FTMD} - \dot{X}_3) |Z|^n \quad (10)$$

in which q is the yield displacement of frictional force loop, and A , β , τ , and n are non-dimensional parameters of the hysteretic loop, which control the shape of the loop. The values of the parameters are adopted in such a way that it provides typical Coulomb-friction damping. The hysteretic displacement component, Z , is bounded by peak values of ± 1 to consider the conditions of sliding and non-sliding phases.

The limited frictional force or slip force, f_s , is stated in a normalized form by a coefficient of friction

$$R_f = \frac{f_s}{M_{FTMD} \cdot g} \quad (11)$$

where M_{FTMD} , g and R_f represent the mass of FTMD, gravitational acceleration and coefficient of friction, respectively.

2.2 Dynamic equations of motion for a seismic-excited structure equipped with FTMD including SSI effects

As can be seen from Fig. 1(b), considering soil-structure interaction effects, two degrees of freedoms, $X_0(t)$ and $\theta_0(t)$, which respectively represent the displacement and rotation of the foundation, should be added to the degrees

of freedoms of the structure.

$$M\ddot{X}(t) + C\dot{X}(t) + KX(t) = -M^*R\ddot{u}_g + BF_s \quad (12)$$

in which M , C , K and M^* denote the mass, damping, stiffness and acceleration mass matrices of the structural system equipped with FTMD including SSI effects, respectively. Using Lagrange's equation, they are given by

$$M = \begin{bmatrix} M_1 & 0 & 0 & 0 & M_1 & M_1 h_1 \\ 0 & M_2 & 0 & 0 & 0 & M_2 h_2 \\ 0 & 0 & M_3 & 0 & 0 & M_3 h_3 \\ 0 & 0 & 0 & M_{FTMD} & M_{FTMD} & M_{FTMD} h_3 \\ M_1 & M_2 & M_3 & M_{FTMD} & M_0 + \sum_{i=1}^3 M_i + M_{FTMD} & \sum_{i=1}^3 M_i h_i \\ M_1 h_1 & M_2 h_2 & M_3 h_3 & M_{FTMD} h_3 & \sum_{i=1}^3 M_i h_i & I_0 + \sum_{i=1}^3 (I_i + M_i h_i^2) + M_{FTMD} h_3^2 \end{bmatrix} \quad (13)$$

$$C = \begin{bmatrix} C_1 + C_2 & -C_2 & 0 & 0 & 0 & 0 \\ -C_2 & C_2 + C_3 & -C_3 & 0 & 0 & 0 \\ 0 & -C_3 & C_3 + C_{FTMD} & -C_{FTMD} & 0 & 0 \\ 0 & 0 & -C_{FTMD} & C_{FTMD} & 0 & 0 \\ 0 & 0 & 0 & 0 & 0 & C_s \\ 0 & 0 & 0 & 0 & 0 & C_r \end{bmatrix} \quad (14)$$

$$K = \begin{bmatrix} K_1 + K_2 & -K_2 & 0 & 0 & 0 & 0 \\ -K_2 & K_2 + K_3 & -K_3 & 0 & 0 & 0 \\ 0 & -K_3 & K_3 + K_{FTMD} & -K_{FTMD} & 0 & 0 \\ 0 & 0 & -K_{FTMD} & K_{FTMD} & 0 & 0 \\ 0 & 0 & 0 & 0 & 0 & K_s \\ 0 & 0 & 0 & 0 & 0 & K_r \end{bmatrix} \quad (15)$$

$$M^* = \begin{bmatrix} M_1 & 0 & 0 & 0 & 0 & 0 \\ 0 & M_2 & 0 & 0 & 0 & 0 \\ 0 & 0 & M_3 & 0 & 0 & 0 \\ 0 & 0 & 0 & M_{FTMD} & 0 & 0 \\ 0 & 0 & 0 & 0 & M_0 + \sum_{i=1}^3 M_i + M_{FTMD} & 0 \\ 0 & 0 & 0 & 0 & 0 & \sum_{i=1}^3 M_i h_i + M_{FTMD} h_3^2 \end{bmatrix} \quad (16)$$

in which M_i , C_i , K_i and I_i represent respectively the mass, damping, stiffness and mass moment of inertia of the i^{th} floor. In addition, h_i ($i=1,2,3$) refers to the height of the i^{th} floor of the structure from the base level. The mass foundation, mass moment of inertia of the foundation are denoted by M_0 and I_0 , respectively. Also, M_{FTMD} , C_{FTMD} and K_{FTMD} are the mass, damping and stiffness of the FTMD. The swaying damping and stiffness of the foundation are also represented by C_s and K_s . Similarly, the rocking damping and stiffness of the foundation are also indicated by C_r and K_r .

In addition, R and B are the location vectors for the seismic excitation and friction force of the FTMD, respectively. Also, $X(t)$, $\dot{X}(t)$ and $\ddot{X}(t)$ represent the relative displacement, velocity and acceleration vectors,

respectively. Considering the studied structure, they are defined as follows

$$\mathbf{R} = [1, 1, 1, 1, 1, 1]^T \quad (17)$$

$$\mathbf{B} = [0, 0, -1, 1, 0, 0]^T \quad (18)$$

$$\mathbf{B} = [0, 0, -1, 1, 0, 0]^T \quad (19)$$

where $X_i(t)$ is the displacement of the i^{th} floor and $X_0(t)$ and $\theta_0(t)$ are the displacement and rotation of the foundation, respectively.

3. An overview of multi-objective particle swarm optimization

PSO as a population-based stochastic optimization algorithm is proposed based on the behavior of swarms in nature such as birds, fish (Kennedy 2011). The status of a particle in the search space can be characterized by two factors: position and velocity. Considering the d -dimensional search space, the position and the velocity of the i th particle can be represented by the vectors $x_i = (x_{i1}, x_{i2}, \dots, x_{id})$ and $v_i = (v_{i1}, v_{i2}, \dots, v_{id})$, respectively. Each particle has its own best position (p_{best}) $p_i = (p_{i1}, p_{i2}, \dots, p_{id})$ corresponding to the personal best objective value obtained so far at time t . The global best particle is also represented as g , which denotes the best position found so far at time t in the whole swarm. The new velocity of each particle and the position of the i -th particle are then updated using Eqs. (20) and (21), respectively (Shi 2001).

$$v_{ij}(t+1) = wv_{ij}(t) + c_1r_1[p_{ij} - x_{ij}(t)] + c_2r_2[g_j - x_{ij}(t)], \quad j = 1, 2, \dots, d \quad (20)$$

$$x_{ij}(t+1) = x_{ij}(t) + v_{ij}(t+1), \quad j = 1, 2, \dots, d \quad (21)$$

where the constants c_1 and c_2 are acceleration coefficients which influence the convergence speed of each particle and are often set to 2.0 according to the past experiences. Furthermore, r_1 and r_2 are two independent random numbers uniformly distributed in the range $[0, 1]$, w is the inertia weight factor which is often in the range $[0.1, 0.9]$ and it can be obtained using the following updated equation for improving the convergence

$$w = w_{max} - n_i \left(\frac{w_{max} - w_{min}}{n_{max}} \right) \quad (22)$$

in which w_{max} and w_{min} are denoted the maximum and minimum weights. Also, n_i and n_{max} is the current generation number and the maximum generation number of generation, respectively (Shi and Ebehart 1998).

Coello Coello and Lechuga (2002) introduced multi-objective particle swarm algorithm (MOPSO) for solving multi-objective optimization problems. MOPSO is based on Pareto dominance, which every non-dominated solution is considered as a new leader. In MOSOP, the non-dominated solutions are stored in a repository. When the particles want to move, a member of the repository is selected as their leader. This leader must be both non-dominated and a member of the repository. Repository members represent

Pareto front and contain non-dominated particles. It is notable that no repository exists in PSO because there is only one objective function, and that is a particle, which represents the best solution. On the other hand, there are several particles in MOPSO, which are non-dominated and are placed in the solution set. The implementation of this algorithm is as follows:

1) The MOPSO parameters are adopted

2) The initial population is created.

3) The best personal experience of each particle is determined. If the new position of the particle dominates the best experience, then the new position will replace the best experience, and if none of them dominate the other one, one of the above positions will be randomly considered as the best experience.

4) Non-dominated members of the population are isolated and stored in the repository.

5) Every particle of the repository selects a leader and flows (i.e. its velocity and position is updated).

6) The best personal experience of each particle is updated.

7) Non-dominated new members are added to the repository.

8) Dominated members of the repository are eliminated.

If the termination condition is not fulfilled, the algorithm will be repeated from step 5.

4. Numerical studies

A three-story shear building equipped with an FTMD situated on the top floor, shown in Fig. 1, is considered for numerical studies. The mass, stiffness, height and moment of inertia of each floor are adopted as $M_i = 30 \times 10^3$ kg, $K_i = 3.46 \times 10^6$ N/m, $h_i = 3.5$ m and $I_i = 1.6 \times 10^5$ kg.m², respectively. To investigate the SSI effects, a rigid circular foundation on the ground surface is adopted. The values of the swaying damping and stiffness of the foundation, and the rocking damping and stiffness of the foundation are dependent on the soil properties include of Poisson's ratio ν , density ρ_s , shear wave velocity V_s and shear modulus G_s and radius of foundation R . They can be given by the following equations (Spyrakos *et al.* 2009).

$$K_s = \frac{8GR}{2-\nu} \quad (23)$$

$$C_s = \frac{4.6}{2-\nu} \rho_s V_s R^2 \quad (24)$$

$$K_r = \frac{8GR^3}{3(1-\nu)} \quad (25)$$

$$C_r = \frac{0.4}{1-\nu} \rho_s V_s R^4 \quad (26)$$

The specifications of the dense, medium and soft soils, considered in this study for investigation SSI effects, are inserted in Table 1. For a vast and practical range of the TMD/FTMD mass ratio, three types of soils include soft, medium and dense soils, as well as the fixed base case, a parametric study based on MOPSO algorithm, is performed

Table 1 The parameters of soil and foundation

Soil type	Poisson's ratio	Soil density (kg/m ³)	Shear-wave velocity (m/s)	Shear modulus (N/m ²)
Dense soil	0.33	2400	500	6.00×10 ⁸
Medium soil	0.48	1900	300	1.71×10 ⁸
Soft soil	0.49	1800	100	1.80×10 ⁷

on the optimum TMD/FTMD parameters include of frequency ratio, damping ratio, and friction coefficient. Furthermore, to compare the performance TMD with FTMD in vibration mitigation of the structure subjected to earthquakes with different intensities and frequencies four well-known earthquakes are also considered in the numerical studies. The numerical studies are carried out for different conditions of ground state.

Optimum design of passive devices for a particular earthquake cannot provide a guarantee to be effective for other earthquakes. Considering seismic events as probabilistic events, it is required several time-consuming analyses to access reliable results in the optimum design process. In order to overcome this problem, an artificial acceleration of the ground motion is simulated for modeling the possible earthquakes (Etedali 2017). It is generated by passing a Gaussian white noise process through the well-known Kanai-Tajimi filter. The power spectral density function of the filter is given by (Mohebbi *et al.* 2013)

$$s(\omega) = S_0 \left[\frac{\omega_g^4 + 4\xi_g^2 \omega_g^2 \omega^2}{(\omega^2 - \omega_g^2)^2 + 4\xi_g^2 \omega_g^2 \omega^2} \right], S_0 = \frac{0.03\xi_g}{\pi\omega_g(4\xi_g^2 + 1)} \quad (27)$$

in which ξ_g and ω_g are the damping ratio and angular frequency of the ground, respectively. In the study, the angular frequencies of the ground considered as $\omega_g = 5, 10$ and 15 rad/sec for soft, medium and dense soils, respectively. The corresponding damping ratios of the ground are adopted as $\xi_g = 0.2, 0.4$ and 0.6 , respectively (Zerva 2016). The output of this filter simulates the earthquake, which has been used for optimum design the of TMD and FTMD devices.

Passive friction devices usually reduce the maximum floor displacement at the cost of an increase in the acceleration of floors. In order to create a good trade-off between the conflicted structural responses, a meta-heuristic multi-objective optimization algorithm based on MOPSO is employed for optimum tuning of TMD and FTMD parameters. For this purposes, two optimization problems are defined for optimum design of TMD and FTMD parameters in the seismic excited structure studied in this paper.

The first optimization problem is defined for optimum design of TMD parameter, including frequency ratio, f_T , and damping ratio, ξ_T , as follows

Find: f_T and ξ_T

$$\text{Minimize } \frac{\max\|X_i(t)\|}{\max\|\hat{X}_i(t)\|} \text{ and } \frac{\max\|\dot{X}_i(t)\|}{\max\|\dot{\hat{X}}_i(t)\|} \quad (i = 1,2,3) \quad (28)$$

Subjected to: $0.6 \leq f_T \leq 1.2, 0.01 \leq \xi_T \leq 0.2$

where $\max\|x_i(t)\|$ and $\max\|\hat{x}_i(t)\|$ represent the maximum floor displacement of the structure equipped with

TMD and the corresponding responses for the structure without TMD.

Similarly, $\max\|\ddot{X}_i(t)\|$ and $\max\|\ddot{\hat{X}}_i(t)\|$ refer to the maximum floor acceleration of the structure equipped with TMD and the corresponding responses for the structure without TMD. Two above normalized responses are considered as objective functions in the design process using MOPSO. To conduct a parametric study, the design process of TMD parameters are carried out for a vast and practical range of the preselected TMD mass ratio $0.01 \leq \lambda \leq 0.1$. For a preselected mass ratio of TMD, λ , the optimum TMD mass, damping and stiffness are calculated as $M_{TMD} = \lambda M_s$, $C_{TMD} = 2M_{TMD}\xi_T f_T \omega_s$ and $K_{TMD} = M_{TMD} f_T^2 \omega_s^2$, in which $M_s = \sum_{i=1}^N M_i$ and ω_s are the total mass and the fundamental frequency of the primary structure.

The second optimization problem is defined for optimum design of FTMD parameter, including frequency ratio f_F , damping ratio ξ_F , and coefficient of friction R_f , as follows

Find: f_F, ξ_F, R_f

$$\text{Minimize } \frac{\max\|X_i(t)\|}{\max\|\hat{X}_i(t)\|} \text{ and } \frac{\max\|\dot{X}_i(t)\|}{\max\|\dot{\hat{X}}_i(t)\|} \quad (i = 1,2,3) \quad (29)$$

Subjected to: $0.6 \leq f_F \leq 1.2, 0.01 \leq \xi_F \leq 0.2, 0.01 \leq R_f \leq 0.5$

in which $\frac{\max\|X_i(t)\|}{\max\|\hat{X}_i(t)\|}$ represents the maximum floor displacement of the structure equipped with FTMD normalized to the corresponding responses for the structure without FTMD. Similarly, $\frac{\max\|\dot{X}_i(t)\|}{\max\|\dot{\hat{X}}_i(t)\|}$ refers to the

maximum floor acceleration of the structure equipped with FTMD normalized to the corresponding responses for the structure without FTMD. The design process of FTMD parameters are done for a vast and practical range of the preselected FTMD mass ratio $0.01 \leq \lambda \leq 0.1$. The optimum FTMD mass, damping and stiffness can then be obtained as $M_{FTMD} = \lambda M_s$, $C_{FTMD} = 2M_{FTMD}\xi_F f_F \omega_s$ and $K_{FTMD} = M_{FTMD} f_F^2 \omega_s^2$, in which $M_s = \sum_{i=1}^N M_i$ and ω_s are the total mass and the fundamental frequency of the primary structure. The slip force, f_s , can be calculated from Eq. (11).

The population size, the initial inertia weight, the final inertia weight, the acceleration constants of the MOPSO algorithm, used for numerical study on optimum parameters of TMD are set as 70, $w_{min} = 0.4$, $w_{max} = 0.9$, $c_1 = c_2 = 2$. Similarly, these parameters are considered as 100, $w_{min} = 0.4$, $w_{max} = 0.9$, $c_1 = c_2 = 2$ for optimum tuning FTMD parameters.

MATLAB/ Simulink software [38] is employed for simulation the nonlinear behavior of force-deformation of the FMFD and time-history analyses of the structure equipped with FTMD. Furthermore, to solve the optimization problems given by Eqs. (28) and (29), an optimization program based on MOPSO is written in MATLAB (2000).

5. Results and discussion

Considering the structure subjected to the artificial

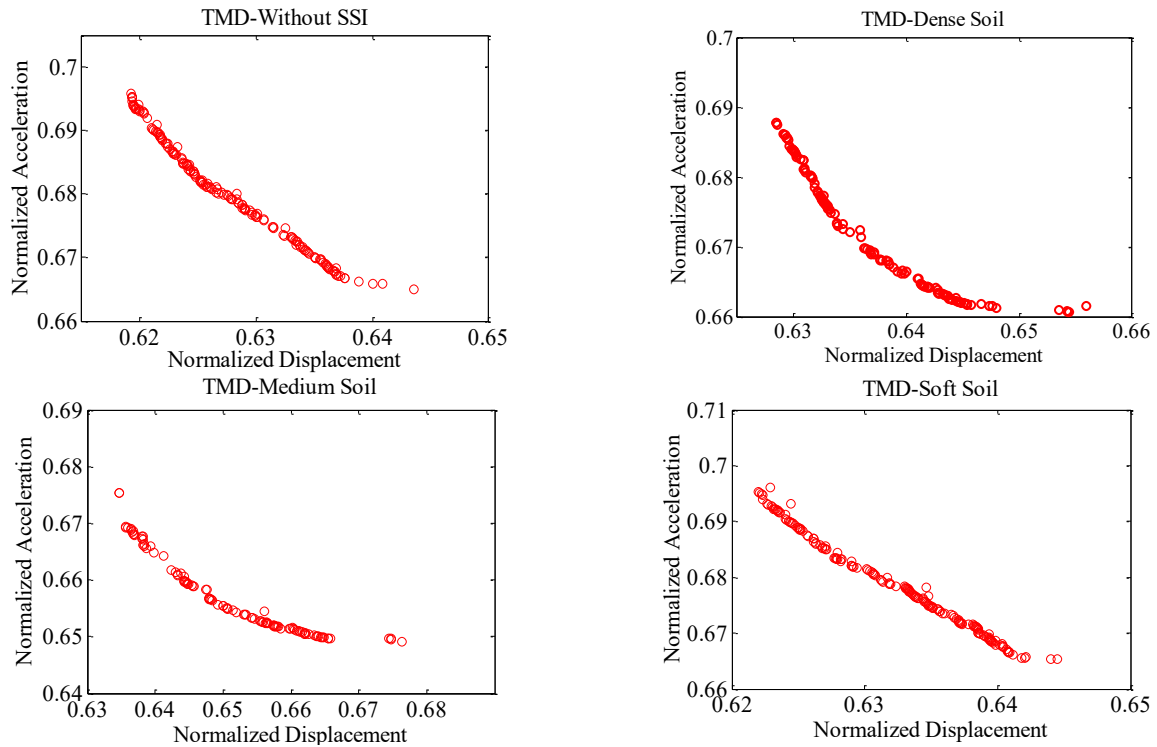


Fig. 2 The Pareto-optimal front diagram for optimum tuning of TMD parameters for $\lambda=0.05$ and different conditions of ground state

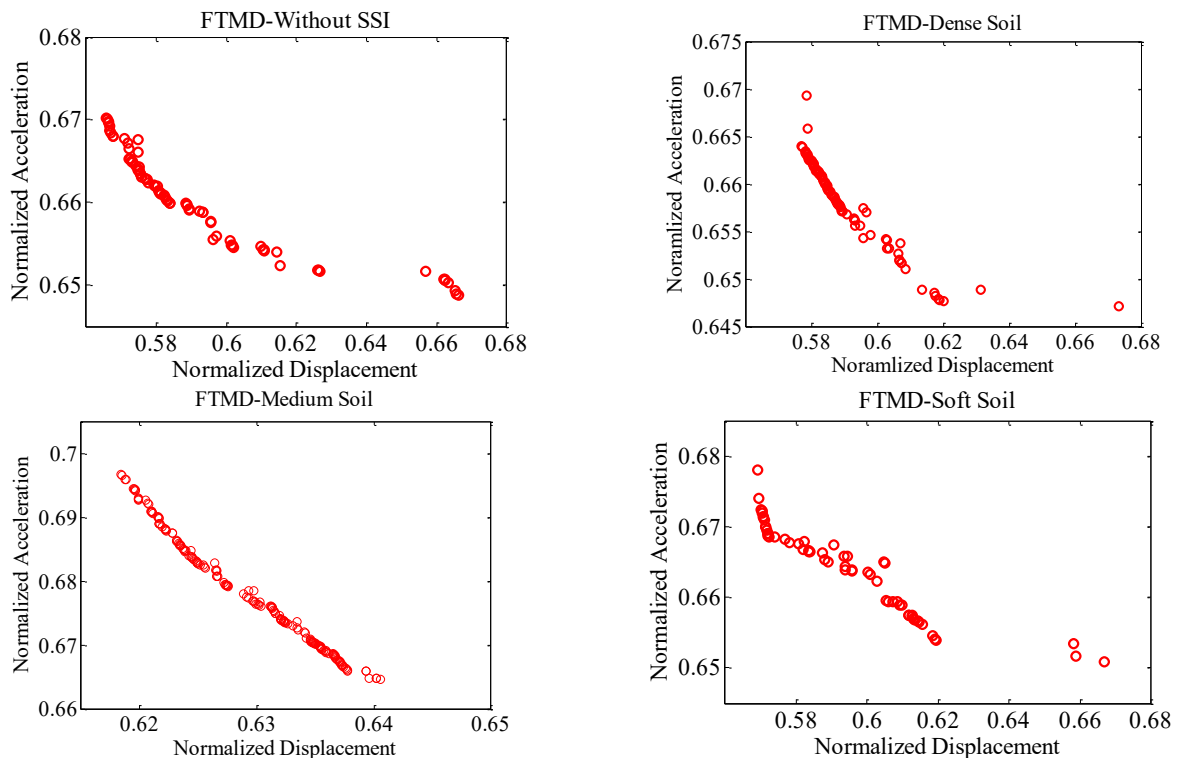


Fig. 3 The Pareto-optimal front diagram for optimum tuning of FTMD parameters for $\lambda=0.05$ and different conditions of ground state

earthquake, the MOPSO algorithm is applied to solve the optimization problems defined for optimum tuning of TMD and FTMD parameters for different preselected of TMD/FTMD mass ratios $\lambda=0.01, 0.02, 0.03, 0.04, 0.05,$

$0.06, 0.07, 0.08, 0.09, 0.1$ and different conditions of ground state. Overall, 80 multi-objective optimum tuning of TMD and FTMD parameters are obtained to carry out a comprehensive numerical study. For example, Fig. 2 shows

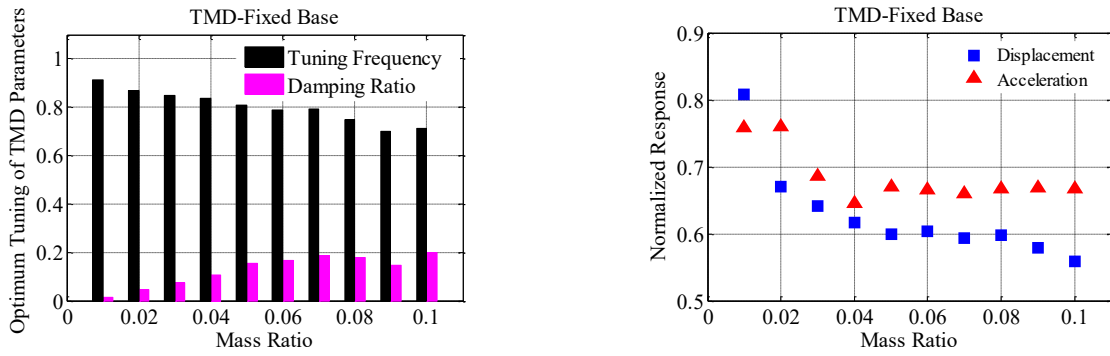


Fig. 4 Optimum TMD parameters for different mass ratios in the case of the fixed base, and the corresponding normalized responses of the structure

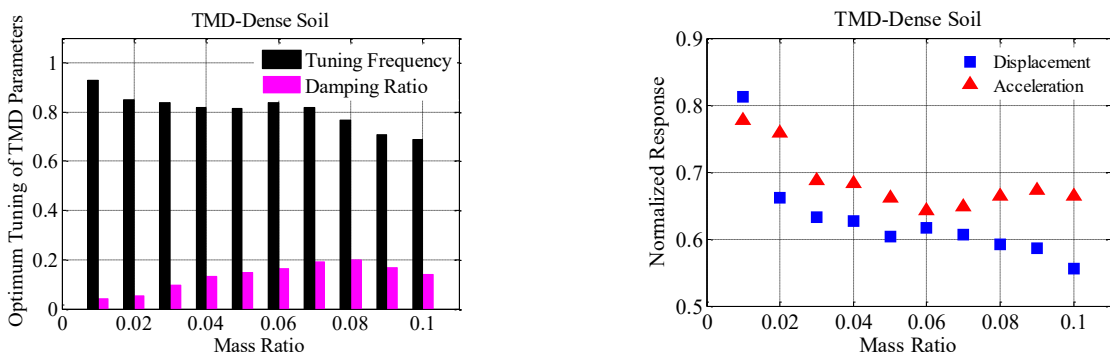


Fig. 5 Optimum TMD parameters for different mass ratios in the case of dense soil, and the corresponding normalized responses of the structure

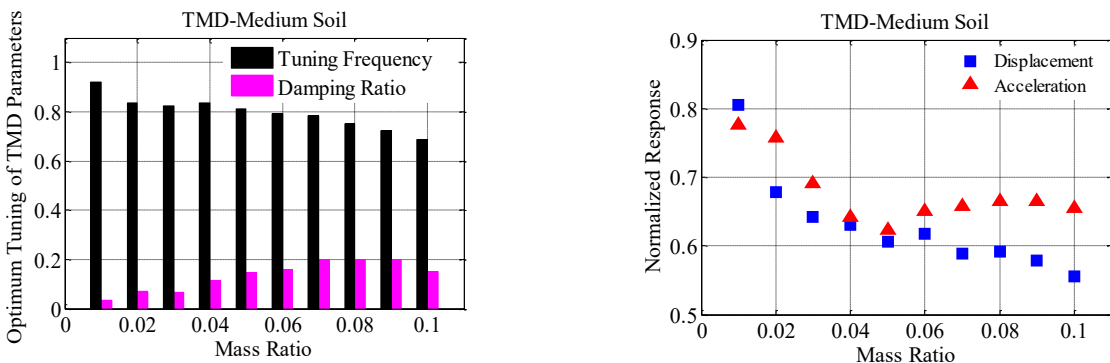


Fig. 6 Optimum TMD parameters for different mass ratios in the case of medium soil, and the corresponding normalized responses of the structure

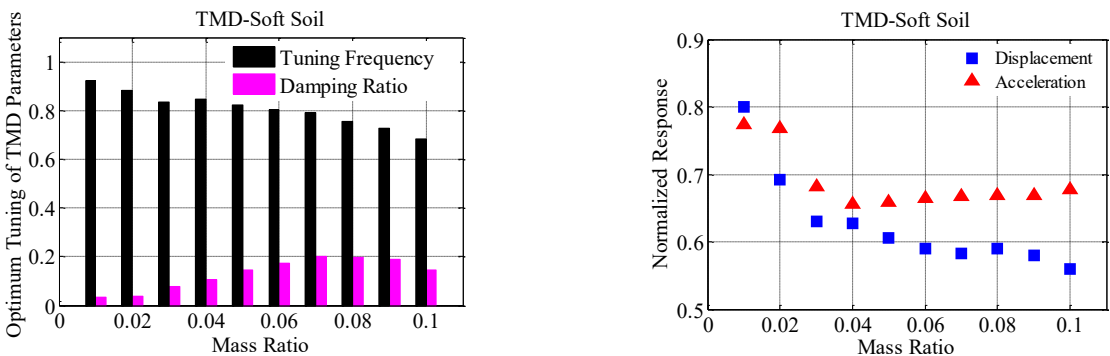


Fig. 7 Optimum TMD parameters for different mass ratios in the case of soft soil, and the corresponding normalized responses of the structure

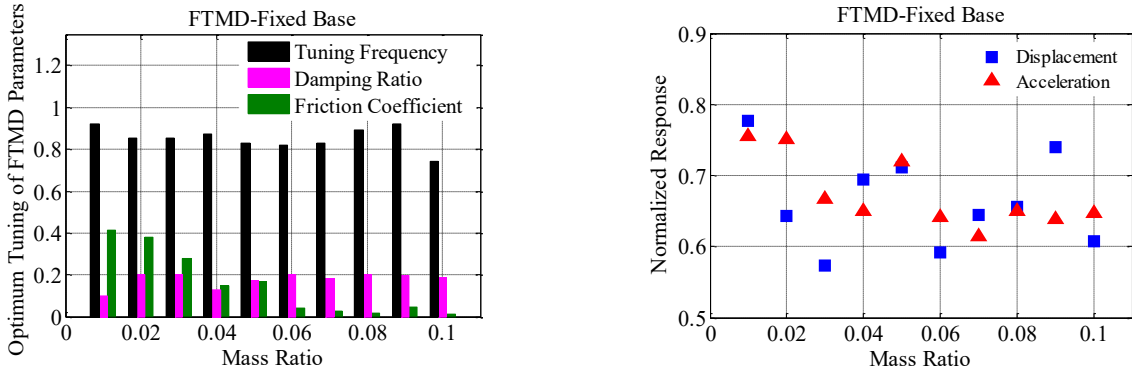


Fig. 8 Optimum FTMD parameters for different mass ratios in the case of the fixed base, and the corresponding normalized responses of the structure

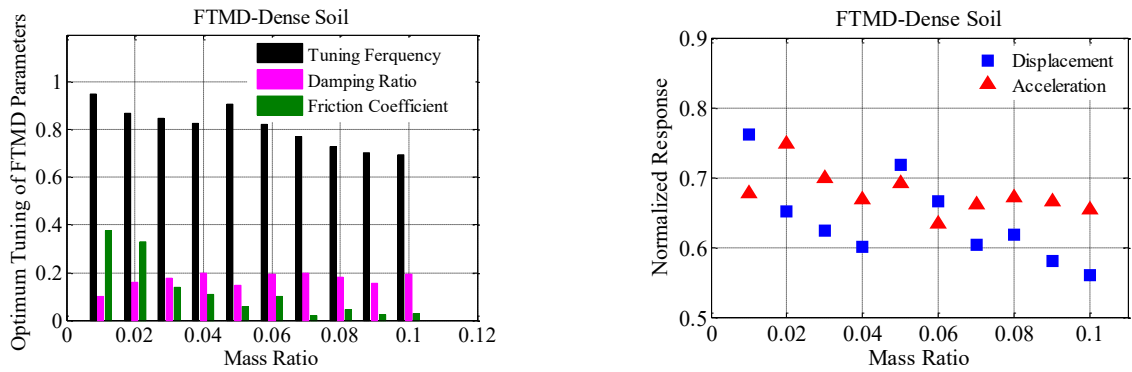


Fig. 9 Optimum FTMD parameters for different mass ratios in the case of dense soil, and the corresponding normalized responses of the structure

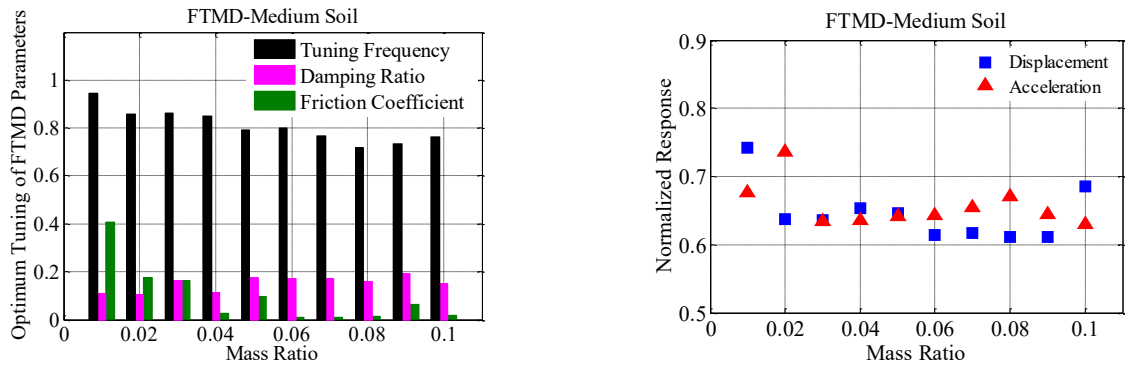


Fig. 10 Optimum FTMD parameters for different mass ratios in the case of medium soil, and the corresponding normalized responses of the structure

the Pareto-optimal front diagrams of MOPSO algorithm for TMD mass ratio $\lambda=0.05$ in the cases of without SSI, dense, medium and soft soils. Similarly, the Pareto-optimal front diagrams for optimum design of FTMD for $\lambda=0.05$ are illustrated in Fig. 3. It is obvious that two objective functions, the normalized responses in the terms of the top floor displacement and acceleration of the structure, are in conflict with each other. MOPSO algorithm is able to create an appropriate trade-off between two conflicting objectives and generates a set of possible solutions for designers that form the so-called Pareto front. Each member of the Pareto front can be represented by a vector in the design space.

The vector that has the shortest distance to the origin is

taken as the best tuning TMD/FTMD parameters.

Fig. 4 illustrates the optimum TMD parameters obtained from MOPSO for different TMD mass ratios in the case of fixed base i.e., the case of without SSI effect. The corresponding normalized responses of the structure are also displayed in the figure. Similarly, the optimum TMD parameters for different mass ratios in the cases of dense, medium and soft soils are shown in Figs. 5-7, respectively. The normalized responses of the structure are also represented in the figures. It is found that by increasing the TMD mass ratio, the optimum tuning frequency ratio is slightly decreased while the optimum-damping ratio often increases. In addition, by increasing the TMD mass ratio, the normalized responses in the term of maximum top floor

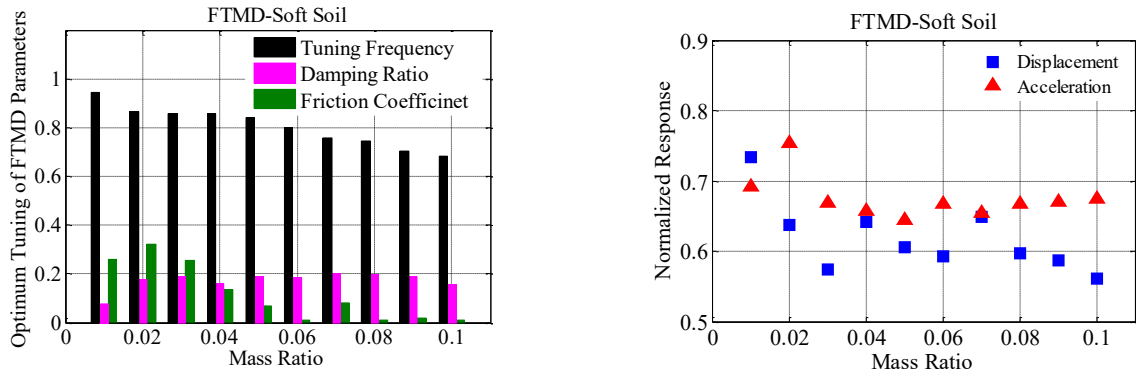


Fig. 11 Optimum FTMD parameters for different mass ratios in the case of soft soil, and the corresponding normalized responses of the structure

Table 2 Optimum TMD and FTMD parameters given by MOPSO algorithm for the case of $\lambda = 0.03$

	TMD		FTMD		
	f_{opt}	ξ_{opt}	f_{opt}	ξ_{opt}	R_{opt}
Without SSI	0.8483	0.0885	0.8546	0.1945	0.2344
Dense Soil	0.8271	0.0914	0.8489	0.1753	0.1397
Medium Soil	0.8243	0.0993	0.8608	0.1647	0.2479
Soft Soil	0.8358	0.0882	0.8589	0.1882	0.2566

Table 3 Maximum seismic responses of the structure subjected to different earthquake excitations

Earthquake	Control case	Soft soil		Medium soil		Dense soil		Fixed base	
		Max Disp. (m)	Max Acc. (m/s ²)	Max. Disp. (m)	Max Acc. (m/s ²)	Max. Disp. (m)	Max Acc. (m/s ²)	Max. Disp. (m)	Max Acc. (m/s ²)
Northridge	Uncontrolled	0.47	14.30	0.47	14.06	0.47	14.28	0.47	14.24
	TMD	0.45 (-4%)	13.79 (-4%)	0.46 (-2%)	13.55 (-4%)	0.45 (-4%)	13.80 (-3%)	0.45(-4%)	13.78 (-3%)
	FTMD	0.39(-17%)*	12.75 (-11%)	0.39 (-17%)	12.45 (-11%)	0.42 (-11%)	13.17 (-8%)	0.38 (-19%)	12.75 (-10%)
Rubakdu	Uncontrolled	0.45	12.13	0.42	11.49	0.44	12.00	0.44	11.82
	TMD	0.33(-26%)	8.22 (-32%)	0.29 (-31%)	7.92 (-31%)	0.29 (-34%)	8.36 (-30%)	0.27 (-39%)	8.00 (-32%)
	FTMD	0.30 (-33%)	8.10 (-33%)	0.25 (-40%)	7.09 (-38%)	0.23 (-48%)	8.14 (-32%)	0.22 (-50%)	7.31 (-38%)
Newhall	Uncontrolled	0.38	10.01	0.37	9.82	0.38	10.03	0.38	10.03
	TMD	0.32 (-17%)	9.80 (-2%)	0.28 (-24%)	9.61 (-2%)	0.28 (-26%)	9.82 (-2%)	0.27 (-29%)	9.82 (-2%)
	FTMD	0.27 (-29%)	9.02 (-10%)	0.24 (-35%)	8.54 (-13%)	0.25 (-34%)	9.29 (-7%)	0.21 (-45%)	8.97 (-11%)
Sylmar	Uncontrolled	0.29	8.25	0.28	8.11	0.29	8.21	0.29	8.21
	TMD	0.25 (-13%)	8.34 (+1%)	0.24 (-14%)	8.19 (+1%)	0.24 (-17%)	8.30 (+1%)	0.24 (-17%)	8.31 (+1%)
	FTMD	0.23 (-20%)	7.98 (-3%)	0.22 (-20%)	7.14 (-12%)	0.20 (-31%)	8.03 (-2%)	0.21 (-28%)	7.82 (-15%)

displacement of the structure experience a decreasing trend, while increasing the TMD mass ratio is not able to provide a significant reduction in the normalized responses of the structure in the term of maximum top floor displacement. It can also be seen that there are slight differences between the optimum parameters of TMD in different conditions of ground state.

Figs. 8-11 show optimum parameters of FTMD and normalized responses of the structure for different ratios of FTMD in the cases of the fixed base, dense soil, medium soil and soft soil, respectively. The results indicate that the SSI influence on the optimum parameters of FTMD. It is also found that by increasing the mass ratio of FTMD, the optimum friction coefficient of the FTMD often decreases.

Unlike TMDs, the seismic performance of the structure equipped with FTMD does not enhance by increasing the mass ratio of FTMD. At lower mass ratios, the FTMDs often perform better than TMD with demand greater optimum friction coefficients in the design process. In the cases, the friction force of the FTMD plays a key role in the reduction of the structural responses of the seismic-excited structure. By increasing the mass ratio of FTMD, the optimum friction coefficient of FTMD is reduced. In the case of large mass ratios, it may be that the FTMDs are not able to slide. Therefore, they demand smaller friction forces for sliding in the optimum design process and may not be able to waste enough energy for the artificial earthquakes. As can be seen, the FTMD for the cases of $\lambda \leq 0.03$

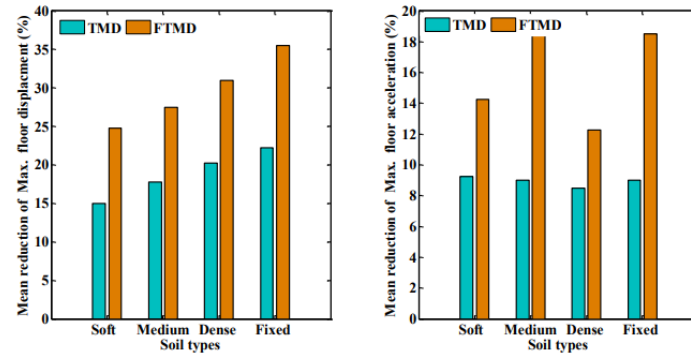


Fig. 12 The mean reduction of maximum floor displacement and acceleration of the structure equipped with TMD and FTMD in comparison with the uncontrolled case for the fixed base and three types of soils

provides a more favorable performance compared with TMD in reduction seismic responses of the structure. As a result, the seismic responses of structures equipped with FTMD are sensitive to the values of optimum FTMD parameters, and unlike TMDs, optimum tuning of FTMD parameters for a large preselected mass ratio may not provide a best and optimum design. On the other hand, for low mass ratios, optimal selection of friction coefficient has an important key to enhance the performance of FTMDs.

The results of the numerical studies on optimum FTMD parameters are shown that the best performance of FTMD in the reduction of the structural responses of the studied structure is given for the FTMD mass ratio $\lambda = 0.03$. For this case, the optimum TMD and FTMD parameters given by MOPSO algorithm are inserted in Table 2. In order to compare the performance of FTMD with TMD in the reduction of the structural responses of the studied structure under real earthquakes with different intensities and frequencies, four well-known earthquake excitations include of Northridge, Rinaldi, Newhall, Sylmar earthquakes, are considered.

Considering the structure on the fixed base and three types of soils, the time history analyses of the structure are carried out subjected to the mentioned earthquake excitations. The seismic responses of the structure, in the cases of the uncontrolled, equipped with TMD and FTMD, are compared in Table 3 for different conditions of ground state. The values inserted in the brackets represent the reduction percentages of the maximum structural responses with respect to the uncontrolled case. The best results are in bold. It is concluded that the performances of TMD and FTMD in the reduction of structural responses of the structure are influenced by the input excitation and type of soil. The TMD mitigates the structural responses in most cases; however, it may not result in a significant effect in some earthquake excitations such as Northridge. In addition, its efficiency is usually reduced in soft soils. For example, TMD results in 17%, 24%, 26% and 29% reduction in peak floor displacement of the structure subjected to Newhall earthquake for the cases of soft, medium, dense soil and fixed base, respectively. TMD is not able to provide a suitable performance in the reduction of the maximum floor acceleration as much as its performance in reducing the maximum floor displacement of the structure. The results show that the FTMDs are advantageous devices for vibration mitigation of the seismic-excited buildings. In comparison with TMD, it is

found that the FTMD provides a better performance in reducing the peak floor displacement and acceleration of the structure in most earthquakes for different conditions of ground state. For example, for Newhall earthquake, FTMD results in 29%, 35%, 34% and 45% reduction in peak top floor displacement for soft, medium, dense and fixed base in comparison with the uncontrolled case. These results show that the FTMD performs better than the TMD in reduction maximum floor displacement of the structure about 16%, 14%, 11% and 22% in Newhall earthquake for the cases of soft, medium, dense soil and fixed base, respectively. Similarly, in comparison with the TMD, the FTMD gives a reduction about 8%, 11%, 5% and 9% in maximum floor acceleration of the structure during Newhall earthquake, respectively. It is also found that the FTMDs are more effective for the dense and hard soil and its efficiency is often reduced in soft soils.

In order to achieve an overall result, the mean reduction of the structural responses for the studied earthquakes in the terms of maximum floor displacement and acceleration are shown in Fig. 12. The results are represented in the cases of three types of soils and the case of fixed base. On average, the TMD is able to reduce the maximum top floor displacement of the structure about 15%, 17.75%, 20.25% and 22.25% for the cases of soft, medium, dense soils, and fixed base conditions, respectively.

Similarly, these reductions are given about 24.75%, 27.5%, 31% and 35.5% for FTMD, respectively. The best results in the reduction of maximum floor displacement for TMD and FTMD are obtained for the fixed base state and their performance decreases with increasing soil softness, so that ignoring the SSI effects in the modeling of the structure may result in incorrect and unrealistic results of the seismic behavior of the structure. It is also seen, on average, the FTMD is able to reduce the maximum top floor acceleration of the structure about 6%, 10%, 5% and 10% better than the TMD for the cases of soft, medium, dense soils, and fixed base conditions. Consequently, the FTMD significantly provides a better performance in reducing the maximum top floor displacement and acceleration of the building in all condition of the ground state.

6. Conclusions

A numerical study on the optimum tuning of parameters of TMD and FTMD include of frequency ratio, damping

ratio and friction coefficient for a vast and practical range of the TMD and FTMD mass ratios was conducted for seismic-excited structures considering SSI effects. Three types of soils include soft, medium and dense soils were considered for investigation the SSI effects on performances TMD and FTMD in comparison with the fixed base case. A MOPSO algorithm as a powerful tool was employed for optimum tuning of the TMD and FTMD parameters. It was found that by increasing the mass ratio of FTMD, the optimum friction coefficient of the FTMD decreases. In other words, for a large mass ratio, the FTMDs were not able to slide and therefore a performance degradation of the FTMD was observed in this case. For a small mass ratio, the friction force of the FTMD played a key role in the reduction of the structural responses of the seismic-excited structure. In this case, the performance of FTMD can enhance by increasing optimum friction coefficient of the FTMD and it was effectively able to waste the input energy. On the other hand, employing an FTMD with a small mass ratio can be an advantage from the standpoint of practical and operational. Hence, it is recommended that a free parameter search of all FTMD parameters, rather than considering a preselected mass ratio for the FTMD was conducted optimum design stage of the FTMD. At the end, the performances of the optimized TMD and FTMD for a 3-story structure were compared with the uncontrolled structure for three types of soils and the fixed base state and four well-known earthquakes. The simulation results showed that the FTMD were able to give a better performance in reducing the maximum top floor displacement and acceleration of the structure in all conditions of the ground state. Furthermore, the results indicated that the SSI significant effected on the optimum design of the TMD and FTMD, so that the performance of the TMD and FTMD decreased with increasing soil softness. Therefore, ignoring the SSI effects in the modeling of the structure may present an unrealistic estimation of the seismic behavior of the structure equipped with TMD and FTMD.

References

- Bakre, S. and Jangid, R. (2007), "Optimum parameters of tuned mass damper for damped main system", *Struct. Control Health Monit.*, **14**(3), 448-470.
- Bekdaş, G. and Nigdeli, S.M. (2017), "Metaheuristic based optimization of tuned mass dampers under earthquake excitation by considering soil-structure interaction", *Soil Dyn. Earthq. Eng.*, **92**, 443-461.
- Brzeski, P., Kapitaniak, T. and Perlikowski, P. (2016), "The use of tuned mass absorber to prevent overturning of the rigid block during earthquake", *Int. J. Struct. Stab. Dyn.*, **16**(10), 1550075.
- Chang, C. (1999), "Mass dampers and their optimal designs for building vibration control", *Eng. Struct.*, **21**(5), 454-463.
- Coello Coello, C.A. and Lechuga, M.S. (2002), "MOPSO: A proposal for multiple objective particle swarm optimization", *Proceedings of the 2002 Congress on Evolutionary Computation (CEC 2002)*, Honolulu, Hawaii, U.S.A., May.
- Constantinou, M., Mokha, A. and Reinhorn, A. (1990), "Teflon bearings in base isolation II: Modeling", *J. Struct. Eng.*, **116**(2), 455-474.
- Etedali S. and Tavakoli S. (2017), "PD/PID controller design for seismic control of high-rise buildings using multi-objective optimization: A comparative study with LQR controller", *J. Earthq. Tsunami*, **11**(3), 1750009.
- Etedali, S. (2017), "A new modified independent modal space control approach toward control of seismic-excited structures", *Bull. Earthq. Eng.*, **15**(10), 4215-4243.
- Etedali, S. and Mollayi, N. (2018), "Cuckoo search-based least squares support vector machine models for optimum tuning of tuned mass dampers", *Int. J. Struct. Stab. Dyn.*, **18**(2), 1850028.
- Etedali, S., Sohrabi, M.R. and Tavakoli, S. (2013), "An independent robust modal PID control approach for seismic control of buildings", *J. Civil Eng Urban.*, **3**(5), 279-291.
- Etedali, S., Zamani, A.A. and Tavakoli, S. (2018), "A GBMO-based PI²D^μ controller for vibration mitigation of seismic-excited structures", *Automat. Constr.*, **87**(C), 1-12.
- Farshidianfar, A. and Soheili, S. (2013), "Ant colony optimization of tuned mass dampers for earthquake oscillations of high-rise structures including soil-structure interaction", *Soil Dyn. Earthq. Eng.*, **51**, 14-22.
- Gewei, Z. and Basu, B. (2011), "A study on friction-tuned mass damper: Harmonic solution and statistical linearization", *J. Vib. Control*, **17**(5), 721-731.
- Gholizad, A. and Ojaghzadeh Mohammadi, S.D. (2017), "Reliability-based design of tuned mass damper using Monte Carlo simulation under artificial earthquake records", *Int. J. Struct. Stab. Dyn.*, **17**(10), 1750121.
- Hadi, M.N. and Arfiadi, Y. (1998), "Optimum design of absorber for MDOF structures", *J. Struct. Eng.*, **124**(11), 1272-1280.
- Heidari, A.H., Etedali, S. and Javaheri-Tafti M.R. (2018), "A hybrid LQR-PID control design for seismic control of buildings equipped with ATMD", *Front. Struct. Civ. Eng.*, **12**(1), 44-57.
- Kaveh, A., Mohammadi, S., Hosseini, O.K., Keyhani, A. and Kalatjari, V. (2015), "Optimum parameters of tuned mass dampers for seismic applications using charged system search", *Iran. J. Sci. Technol. Trans. Civ. Eng.*, **39**(C1), 21-40.
- Kennedy, J. (2011), *Particle Swarm Optimization*, in *Encyclopedia of Machine learning*, Springer, Boston, Massachusetts, U.S.A., 760-766.
- Keshtegar, B. and Etedali, S. (2017), "Novel mathematical models based on regression analysis scheme for optimum tuning of TMD parameters", *J. Solid Fluid Mech.*, **6**(4), 59-75.
- Khatibinia, M., Gholami, H. and Labbafi S. (2016), "Multi-objective optimization of tuned mass dampers considering soil-structure interaction", *Int. J. Optim. Civ. Eng.*, **6**(4), 595-610.
- Lee, C.L., Chen, Y.T., Chung, L.L. and Wang Y.P. (2006), "Optimal design theories and applications of tuned mass dampers", *Eng. Struct.*, **28**(1), 43-53.
- Leung, A. and Zhang, H. (2009), "Particle swarm optimization of tuned mass dampers", *Eng. Struct.*, **31**(3), 715-728.
- Lin, C.C., Lin, G.L. and Chiu, K.C. (2017), "Robust design strategy for multiple tuned mass dampers with consideration of frequency bandwidth", *Int. J. Struct. Stab. Dyn.*, **17**(1), 1750002.
- MATLAB (2000), *The MathWorks, Inc.*, Natick, Massachusetts, U.S.A.
- Mohebbi, M., Shakeri, K., Ghanbarpour, Y. and Majzoub, H. (2013), "Designing optimal multiple tuned mass dampers using genetic algorithms (GAs) for mitigating the seismic response of structures", *J. Vib. Control*, **19**(4), 605-625.
- Pisal, A.Y. and Jangid, R. (2014), "Seismic response of multi-story structure with multiple tuned mass friction dampers", *Int. J. Adv. Struct. Eng.*, **6**(1), 46.
- Ricciardelli, F. and Vickery, B.J. (1999), "Tuned vibration absorbers with dry friction damping", *Earthq. Eng. Struct. Dyn.*, **28**(7), 707-723.
- Sadek, F., Mohraz, B., Taylor, A.W. and Chung R.M. (1997), "A method of estimating the parameters of tuned mass dampers for

- seismic applications”, *Earthq. Eng. Struct. Dyn.*, **26**(6), 617-636.
- Salvi, J. and Rizzi, E. (2012), “A numerical approach towards best tuning of tuned mass dampers”, *Proceedings of the 25th International Conference on Noise and Vibration Engineering*, Leuven, Belgium, September.
- Shi, Y. (2001), “Particle swarm optimization: Developments, applications and resources”, *Proceedings of the 2001 Congress on Evolutionary Computation*, Seoul, South Korea, May.
- Shi, Y. and Eberhart, R. (1998), “A modified particle swarm optimizer”, *Proceedings of the IEEE World Congress on Computational Intelligence*, Anchorage, Alaska, U.S.A., May.
- Shourestani, S., Soltani, F., Ghasemi, M. and Etedali, S. (2018), “SSI effects on seismic behavior of smart base-isolated structures”, *Geomech. Eng.*, **14**(2), 161-174.
- Spyrakos, C., Maniatakis, C.A. and Koutromanos, I. (2009), “Soil-structure interaction effects on base-isolated buildings founded on soil stratum”, *Eng. Struct.*, **31**(3), 729-737.
- Tsai, H.C. and Lin, G.C. (1993), “Optimum tuned-mass dampers for minimizing steady-state response of support-excited and damped systems”, *Earthq. Eng. Struct. Dyn.*, **22**(11), 957-973.
- Warburton, G. (1982), “Optimum absorber parameters for various combinations of response and excitation parameters”, *Earthq. Eng. Struct. Dyn.*, **10**(3), 381-401.
- Wen, Y.K. (1976), “Method for random vibration of hysteretic systems”, *J. Eng. Mech. Div.*, **102**(2), 249-263.
- Zerva, A. (2016), *Spatial Variation of Seismic Ground Motions: Modeling and Engineering Applications*, CRC Press.